V.V. ROMAKA,[1] V.A. ROMAKA,[2] Y.V. STADNYK,[3] L.P. ROMAKA,[3]
P.Y. DEMCHENKO,[3] V.Z. PASHKEVYCH,[2] A.M. HORYN[3]

[1] Technische Universität Dresden
(Bergstrasse 66, 01069 Dresden, Germany; e-mail: vitaliy.romaka@tu-dresden.de)
[2] Lviv Polytechnic National University
(12, Bandera Str., Lviv 79013, Ukraine)
[3] Ivan Franko National University of Lviv
(6, Kyryla and Mefodiya Str., Lviv 79005, Ukraine)

FEATURES OF MECHANISMS OF ELECTRICAL CONDUCTIVITY IN SEMICONDUCTIVE SOLID SOLUTION $Lu_{1-x}Sc_xNiSb$

UDC 539

A comprehensive study of the crystal and electronic structures, thermodynamic, electrokinetic, energy, and magnetic properties of the semiconductive solid solution $Lu_{1-x}Sc_xNiSb$, $x = 0$–0.10, revealed the possibility of doping Sc atoms of different crystallographic sites depending on their concentration. This leads to the generation of structural defects of donor and/or acceptor nature and the appearance of the corresponding energy levels (bands) in the band gap ϵ_g. The ratio of ionized donors and acceptors (degree of compensation) determines the position of the Fermi level ϵ_F in $Lu_{1-x}Sc_xNiSb$. The dependence of the rate of generation of energy levels and the position of the Fermi level ϵ_F on the impurity concentration Sc, which determines the mechanism of electrical conductivity of $Lu_{1-x}Sc_xNiSb$, is established. The investigated $Lu_{1-x}Sc_xNiSb$ solid solution is a promising thermoelectric material.

K e y w o r d s: electrical conductivity, thermopower coefficient, Fermi level, semiconductor.

1. Introduction

The promising classes of semiconductor thermoelectric materials with high efficiency of conversion of the thermal energy into the electricity are half-Heusler phases RNiSb and substitutional solid solutions based on them (R – rare earth metal). X-ray diffraction studies of ternary phases in R–Ni–Sb systems have shown the existence of equiatomic compounds [1–3], which, for the case of light rare earth metals (Ce, Pr, Nd, Sm), crystallize in two structure types – AlB_2 and Ni_2In. Instead, the half-Heusler phases of RNiSb with rare-earth metals of the yttrium subgroup crystallize in the structure type of MgAgAs (space group $F\bar{4}3m$). GdNiSb antimonide exists in two structural modifications – high-temperature one with hexagonal structure (structure type AlB_2) and low- temperature modification – structure type MgAgAs [4].

Investigations of the electrokinetic properties of the half-Heusler phases RNiSb (R–Y, Gd–Lu) have shown that they are semiconductors of the hole-type conductivity. X-ray diffraction studies of RNiSb and solid solutions based on them showed that their crystal structure is defective: in $4a$ crystallographic positions of R atoms and $4c$ positions of Ni atoms, there are vacancies – structural defects of acceptor nature, which generate corresponding acceptor levels (bands) in the band gap ϵ_g [5–9]. This is confirmed by positive values of the thermopower coefficient $\alpha(T, x)$.

The presence of vacancies in the 4*a* and 4*c* positions of the half-Heusler RNiSb phases fundamentally changes the mechanisms of entry of other atoms into the crystal structure during the formation of solid solutions. This, in turn, affects the electronic structure and electrokinetic properties. Thus, the formation of semiconductive solid solutions $Er_{1-x}Zr_xNiSb$, x = 0–0.10, and $Lu_{1-x}Zr_xNiSb$, x = 0–0.10, by substituting $Er(5d^06s^2)$ or $Lu(5d^16s^2)$ atoms in the 4*a* crystallographic position by $Zr(4d^25s^2)$ atoms was accompanied by the anomalous behavior of the unit cell parameter $a(x)$. Despite the fact that the atomic radius of $Zr(r_{Zr} = 0.160$ nm) is smaller than the radii of the atoms $Er(r_{Er} = 0.176$ nm) and $Lu(r_{Lu} = 0.173$ nm), X-ray diffraction studies of $Er_{1-x}Zr_xNiSb$ and $Lu_{1-x}Zr_xNiSb$ found that the unit cell parameter $a(x)$ at the concentration x = 0–0.02 increases, passes through the maximum, and decreases at $x > 0.02$. This behavior of $a(x)$ indicates more complex structural changes than the elementary substitution of Er(Lu) atoms by Zr. This, in turn, is reflected in the behavior of the electrokinetic characteristics of $Er_{1-x}Zr_xNiSb$ and $Lu_{1-x}Zr_xNiSb$.

Thus, studies of the electrokinetic and energy properties of $Er_{1-x}Zr_xNiSb$ and $Lu_{1-x}Zr_xNiSb$ in the interval x = 0–0.10 established the anomalous behavior of the resistivity $\rho(x,T)$, thermopower coefficient $\alpha(T,x)$, and Fermi energy ϵ_F. Conduction metallization occurs even at the lowest concentration of Zr atoms ($x = 0.01$), and negative values of the thermopower coefficient $\alpha(T,x)$ indicate the transition of the Fermi level ϵ_F from the band gap ϵ_g to the conduction band ϵ_C [5–8]. This behavior of electrokinetic and energy properties is due to changes in the crystal and electronic structures of $Er_{1-x}Zr_xNiSb$ and $Lu_{1-x}Zr_xNiSb$. In particular, the substitution of Er or Lu atoms by Zr ones in 4*a* position generates structural defects of donor nature, since Zr has a larger number of *d*-electrons than rare earth metal atoms. In this case, an impurity donor band ϵ_D^1 appears in the band gap ϵ_g. In turn, the occupation of vacancies in 4*a* position of Er or Lu atoms by Zr ones simultaneously eliminates structural defects of acceptor nature generated by vacancies and generates defects of donor nature and donor band ε_D^2. The occupation of vacancies by Zr atoms in position 4*c* of Ni atoms simultaneously eliminates structural defects of acceptor nature and generates defects of donor nature and donor band ε_D^3. The period of the unit cell $a(x)$ increases, because the atomic radius of Zr is much larger than that of Ni ($r_{Ni} = 0.124$ nm).

Instead, in a solid solution of $Er_{1-x}Sc_xNiSb$, x = = 0–0.10, the substitution of Er atoms by Sc ($3d^14s^2$), which are located in the same group of the Periodic Table, leads to a decrease in the unit cell period $a(x)$ ($r_{Sc} = 0.164$ nm). The occupation of vacancies in 4*a* position of Er atoms by Sc ones simultaneously eliminates structural defects of acceptor nature and generates defects of neutral nature. The solid solution $Er_{1-x}Sc_xNiSb$ is a semiconductor of the hole-type conductivity at all investigated temperatures [9].

Our long-term X-ray diffraction studies of ternary phases in systems of rare earth metals, transition *d*-metals with tin and antimony have shown the importance of testing the existence of substitutional solid solutions by other methods. Simulations of the change in free energy $\Delta G(x)$ and the enthalpy of mixing ΔH_{mix} for the ordered variant of the structure $Er_{1-x}Zr_xNiSb$, $Lu_{1-x}Zr_xNiSb$ and $Er_{1-x}Sc_xNiSb$ showed [5–9] that the formation of a substitutional solid solution is energetically expedient only at concentrations x = 0–0.10. At higher concentrations, the stratification occurs (spinoidal decay of the phase). The lack of thermodynamic studies of the solid solution of $Tm_{1-x}Sc_xNiSb$ [10] did not allow one to correctly describe the objects of study, as it is impossible to detect the spinoidal decay of a phase only by X-ray methods.

The studied half-Heusler phases RNiSb (R–Y, Gd–Lu) are synthesized by melting the charge of the initial components with subsequent cooling of the melt, which, in particular, is one of the ways to obtain amorphous solids [11]. The synthesis of semiconductive solid solutions based on half-Heusler phases additionally generates structural defects of donor and/or acceptor nature, and the corresponding energy levels (bands) appear in the band gap. Therefore, according to the method of obtaining such thermoelectric material is heavily doped and highly compensated semiconductor (HDHCS) [12].

B. Shklovsky and A. Efros showed that the presence of a significant number of different charged defects in the semiconductor, the location of which is fluctuating, radically changes its electronic structure and leads to fluctuations in potential relief and modulation of continuous energies bands [12]. At low temperatures, a heavily doped crystalline semiconductor is a disordered system that resembles amorphous sys-

tems. The electron is considered not in the periodic field of the crystal, but in the chaotic field of defects. It is the understanding of the nature of structural disorders of the half-Heusler phases, as well as disorders caused by fluctuations in charged impurities, allowed the authors [13] to develop approaches to the physics of heavily doped and highly compensated semiconductor. It was shown that the values of activation energies ϵ_1^α and ϵ_3^α, calculated from high- and low-temperature activation parts of the thermopower coefficient $\alpha(1/T)$, are proportional to the amplitude of modulation of continuous energy bands and small-scale fluctuations of semiconductor, respectively.

Using approaches [12–14] to describe disordered systems, which are semiconductor thermoelectric materials based on half-Heusler phases, the mechanisms of electrical conductivity of solid solution $Lu_{1-x}Sc_xNiSb$, $x = 0$–0.10, formed by substituting Lu atoms in $4a$ position by Sc ones. The following results of studies of structural, thermodynamic, electrokinetic, energy and magnetic properties of $Lu_{1-x}Sc_xNiSb$, $x = 0$–0.10, and the half-Heusler phase ScNiSb will identify factors that have a decisive effect on crystal and electronic structures. This will allow modeling and obtaining thermoelectric materials with high efficiency of conversion of thermal energy into electricity.

2. Experimental

The samples were synthesized by melting the charge components in an electric arc furnace in an inert argon atmosphere followed by homogenizing annealing for 720 h at 1073 K. Diffraction data sets were obtained using a STOE STADI P powder diffractometer (CuKα_1-radiation). Crystallographic parameters were calculated using the Fullprof program [15]. The chemical and phase compositions of the samples were monitored by energy-dispersive X-ray spectroscopy (scanning electron microscope TESKAN VEGA 3 LMU). Calculations of DOS, thermodynamic and energy characteristics were performed by two methods: Korringa–Kohn–Rostoker (KKR) in local density approximation for exchange-correlation potential with Moruzzi, Janak, Williams parameterization [16] and the full-potential method of linearized plane waves (FLAPW) in generalized gradient approximation. Simulations using the KKR method were performed using the AkaiKKR software package [17], and the FLAPW method using the Elk software package [18]. The simulation was performed for a $10\times10\times10$ k-grid, and the Brillouin zone was divided into 1000 k-points, which were used to calculate the Bloch spectral function and the distribution of density of electronic states. The width of the energy window was chosen so as to capture the semi-core states of the p-elements. Accuracy of Fermi energy position calculations $\epsilon_F \pm 6$ meV. Temperature and concentration dependences of resistivity (ρ) and thermopower coefficient (α) were measured with respect to copper and specific magnetic susceptibility (χ) (Faraday method) of samples of solid solution $Lu_{1-x}Sc_xNiSb$, $x = 0$–0.10, and ScNiSb in range $T = 80$–400 K.

3. Results and Discussion

3.1. Investigation of structural and thermodynamic properties

X-ray phase and structural analyzes showed that the powder diffraction patterns of samples $Lu_{1-x}Sc_xNiSb$, $x = 0$–0.10, and ScNiSb are indexed in the MgAgAs structure type and do not contain traces of other phases. Investigations have shown a decrease of the unit cell parameter $a(x)$ with increasing impurity concentration (Fig. 1, *b*). The obtained result was predicted because the atomic radius of Lu is larger than that of Sc. Due to the fact that the Lu and Sc atoms are located in the same group of the Periodic Table of the Elements, the structural defects of neutral nature should be formed in the crystal structure of $Lu_{1-x}Sc_xNiSb$. In this case, the hole conductivity type $Lu_{1-x}Sc_xNiSb$ will be unchanged, and in the experiment we obtain positive values of thermopower coefficient $\alpha(T, x)$.

However, a detailed analysis of the behavior of the lattice parameter $a(x)$ for $Lu_{1-x}Sc_xNiSb$, $x = 0$–0.10, shows that it does not change according to the linear law (Fig. 1, *b*), as expected when Lu atoms are replaced by Sc atoms in $4a$ position. This should indicate that the structure of $Lu_{1-x}Sc_xNiSb$ is undergoing more complex changes, in particular, due to the partial occupation of vacancies by Sc atoms in positions $4a$ and/or $4c$. But the accuracy of X-ray methods does not allow to identify these changes.

Given the existence of a continuous solid solution and an ordered variant of the crystal structure $Lu_{1-x}Sc_xNiSb$, $x = 0$–1.0, the variation in the values of the unit cell parameter $a(x)$ was calculated us-

ing the software packages AkaiKKR [16] and Elk [17] (Fig. 1, *a*, insert). The obtained results are consistent with the experimental data of X-ray structural studies regarding the reduction of the values of the unit cell parameter $a(x)$. It is important to get an answer to the question, does the $Lu_{1-x}Sc_xNiSb$ substitutional solid solution exist at all, and if so, up to what extent? In other words, is the formation of a substitution solution energetically expedient?

Modeling of thermodynamic characteristics for a hypothetical solid solution $Lu_{1-x}Sc_xNiSb$, $x = 0$–1.0 within DFT allows to establish the energy feasibility of the existence of a substitutional solid solution. For this purpose, the FLAPW and KKR methods were used to calculate the change in the enthalpy of mixing $\Delta H_{\text{mix}}(x)$ $Lu_{1-x}Sc_xNiSb$, $x = 0$–1.0, (Fig. 1, *b*).

The calculation by the FLAPW method (Elk software package) shows that the enthalpy of mixing in the whole concentration range is positive indicating that at a very low temperature a substitution of Lu by Sc is thermodynamically impossible. However, the low absolute values of the enthalpy of mixing are easily compensated by the entorpy of mixing term at moderate and high temperatures, pushing the thermodynamic potential to negative values and thus stabilizing the $Lu_{1-x}Sc_xNiSb$, $x = 0$–0.10 solid solution. In addition, the formation of the ScNiSb compound is energetically favorable, which is confirmed by X-ray diffraction studies [19].

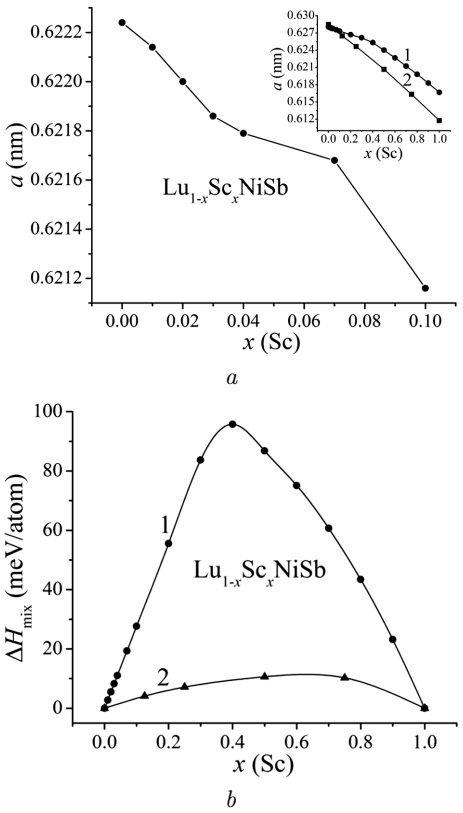

Fig. 1. Variation of the unit cell parameter $a(x)$ (*a*) and the enthalpy of mixing ΔH_{mix} (*b*) $Lu_{1-x}Sc_xNiSb$: KKR method (*1*), FLAPW method (*2*). Insert (*a*): simulation $a(x)$, KKR method (*1*), FLAPW method (*2*)

3.2. Electronic structure modeling

To model the behavior of Fermi energy ϵ_F, band gap ϵ_g, electroinetic characteristics of $Lu_{1-x}Sc_xNiSb$, the distribution of density of electronic states (DOS) for the ordered and disordered variants of the crystal structure was calculated. To understand the mechanism of transformation of the electronic structure of the semiconductor solid solution $Lu_{1-x}Sc_xNiSb$, $x = 0$–0.10, it is important to consider the electronic structure of the basic compound LuNiSb, in which the ratio of structural defects of acceptor and donor nature plays a decisive role. In Fig. 2, *a*, as an example, the results of DOS calculations (software package AkaiKKR [16]) for an ordered variant structure of the half-Heusler phase LuNiSb, in which all crystallographic positions are occupied by atoms according to the MgAgAs structure type, are showed. The simulation exhibits that the LuNiSb compound is a semiconductor of the electron conductivity type, because the Fermi level ϵ_F (dotted line) is located near the conduction band ϵ_C. In this case, electrokinetic studies should obtain negative values of the thermopower coefficient $\alpha(T)$ at all temperatures. This result corresponds to the results of calculations [6], but does not agree with the results of experimental studies [1, 7], where positive values of the thermopower coefficient $\alpha(T)$ were obtained. Therefore, the crystal structure of LuNiSb is not ordered.

The DOS calculation for the disordered variant of the crystal structure of LuNiSb half-Heusler phase was performed using the model we proposed in the DOS calculations for the YNiSb compound [3] (Fig. 2, *b*). A model of the structure of the LuNiSb compound, which can be described by the formula $Lu_{1+y}Ni_{1-2y}Sb$, is considered. In this model, the Lu atoms partially move to the 4*c* position of the Ni atoms, and in this position the vacancies (y) occur

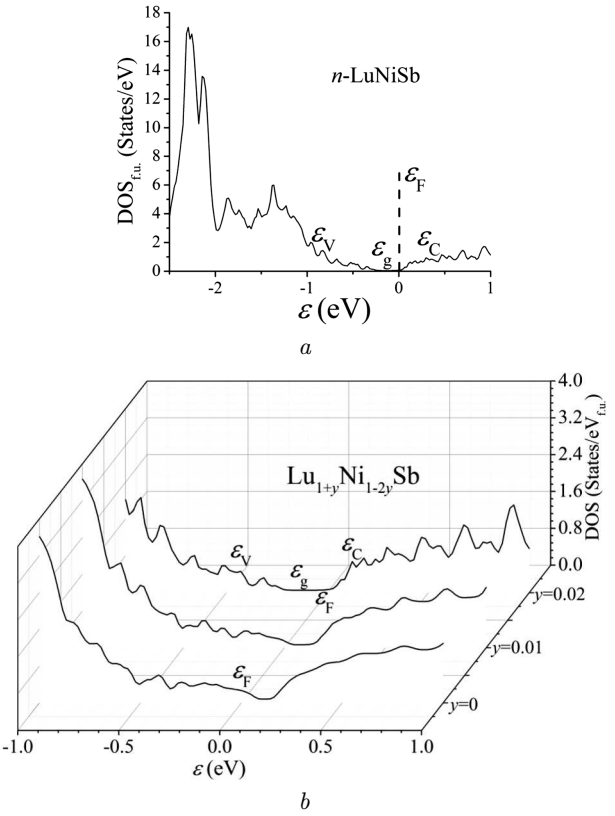

Fig. 2. DOS distribution for ordered (a) and disordered (b) variants of the LuNiSb crystal structure

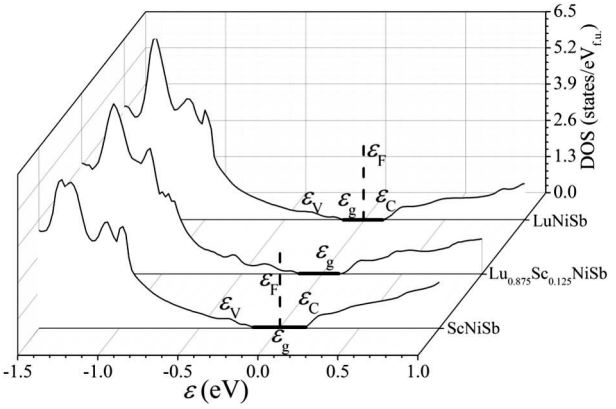

Fig. 3. DOS distribution (FLAPW method) for the ordered variant of the $Lu_{1-x}Sc_xNiSb$ crystal structure

simultaneously. Moreover, as many Lu atoms additionally move to the 4c position of Ni atoms, so many vacancies arise in this position. That is, if the Lu atoms at the number $y = 0.01$ move to the position 4c of the Ni atoms, then there are additional vacancies with a concentration of 0.01. Therefore, in position 4c of Ni atoms there are: Ni – 0.98, Lu – 0.01, Vac – $y = 0.01$. In this model of the crystal structure of the LuNiSb compound, in the absence of vacancies ($y = 0$), the calculation of the DOS electronic state density distribution shows the presence of the band gap ϵ_g, and the Fermi level ϵ_F lies near the valence band ϵ_V (Fig. 2, b). Under such conditions, we obtain positive values of the thermopower coefficient $\alpha(T, x)$ LuNiSb at all investigated temperatures. However, even at concentration $y = 0.02$, the DOS calculation shows that the Fermi level ϵ_F now lies near the conduction band ϵ_C. This means that the main carriers of the electric current of the LuNiSb half-Heusler phase are electrons, which contradicts the results of the experiment [7]. Recall that Ni atoms make the greatest contribution to the formation of the conduction band ϵ_C of the semiconductor.

Based on the assumption that the crystal structure of the semiconductor solid solution $Lu_{1-x}Sc_xNiSb$ is ordered, the distribution of DOS was simulated using the Elk software package [17] (Fig. 3).

It is seen that in LuNiSb the Fermi level ϵ_F lies in the middle of the band gap ϵ_g, which is characteristic of intrinsic semiconductors [12], and the band gap width $\epsilon_g = 190.5$ meV. The DOS simulation results for the ordered variant of $Lu_{0.875}Sc_{0.125}NiSb$ and ScNiSb crystal structure show the DOS redistribution (Fig. 3) and an increase of the band gap ϵ_g. In this case, the Fermi level ϵ_F further lies in the middle of the band gap ϵ_g, because the generated structural defects are neutral in nature. DOS simulation for the ScNiSb half-Heusler phase ($Lu_{1-x}Sc_xNiSb$ at $x = 1.0$) gives a band gap $\epsilon_g = 247.6$ meV, which is greater than that of LuNiSb. In this case, the Fermi level ϵ_F also lies in the middle of the band gap ϵ_g.

Therefore, DOS calculations for the ordered variant of $Lu_{1-x}Sc_xNiSb$ structure do not agree with the experimental results [1, 2, 7].

Calculations of the electron state density distribution for the disordered variant of the $Lu_{1-x}Sc_xNiSb$ structure were performed on the basis of the model used above for the disordered variants of the structure of LuNiSb half-Heusler phase [3]. A model of the structure of semiconductive solid solution $Lu_{1-x+y}Sc_xNi_{1-2y}Sb$ is considered, in which at 4a position Lu atoms are replaced by Sc atoms. In addition, the Lu atoms partially move to the 4c position of the Ni atoms, and in this position the vacan-

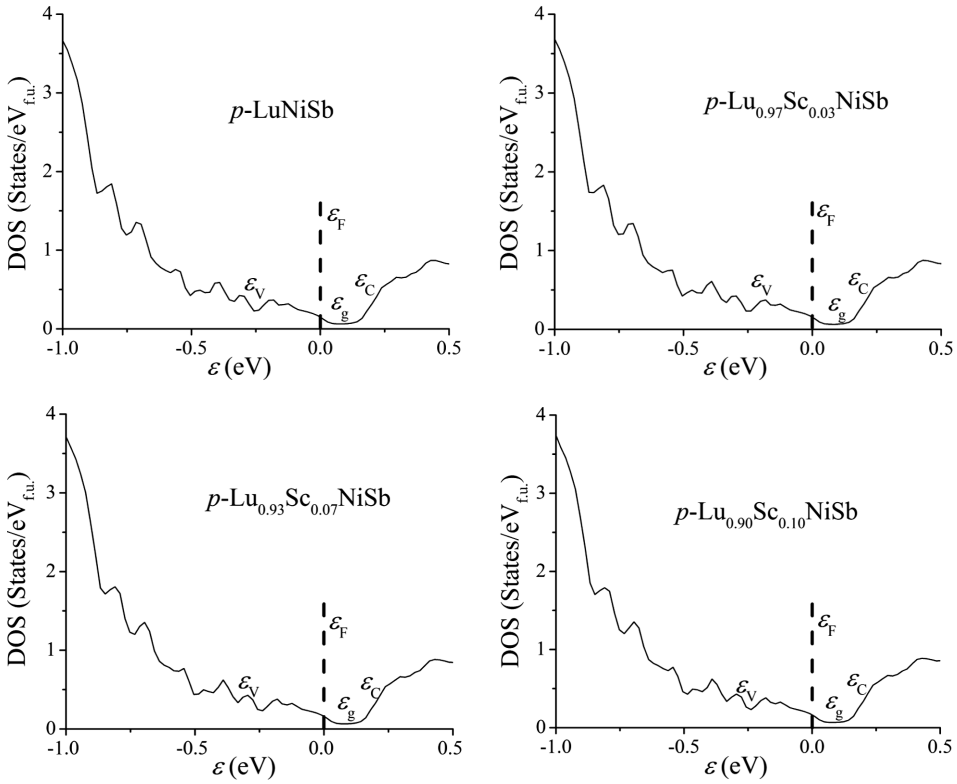

Fig. 4. DOS calculation for the disordered variant of the $Lu_{1-x}Sc_xNiSb$ crystal structure

cies (y) arise at the same time. Moreover, as many Lu atoms additionally move to the 4*c* position of Ni atoms, so many vacancies arise in this position. In this model of the $Lu_{1-x}Sc_xNiSb$ crystal structure, the DOS calculation shows the presence of the band gap ϵ_g (Fig. 4). In this case, structural defects of donor, acceptor and neutral nature occur in the crystal. It is clear that this model is correct for a small number of Sc atoms, because even partial occupation of the 4*c* position of Ni atoms by Lu atoms deforms the structure with its subsequent decay. The disadvantage of this model is also the generation of a significant number of energy levels in the band gap ϵ_g, which intersect with the continuous energies bands of semiconductor and fix the Fermi level ϵ_F (Fig. 4). This makes it difficult to determine the band gap ϵ_g and the activation energy $\epsilon_1^\rho(x)$ from the Fermi level ϵ_F to the valence band ϵ_V.

On the other hand, the hole type of conductivity for $Lu_{1-x}Sc_xNiSb$ means that the concentration of acceptors predominates over donors in the semiconductor. Previous studies [6–8] have shown that in the case of LuNiSb the Fermi level ϵ_F is located at a distance of 10.2 meV from the top of the valence band ε_V, and the amplitude of modulation of the continuous energies bands is $\epsilon_1^\alpha = 35.7$ meV. For ScNiSb, the Fermi level ϵ_F lies at a distance $\epsilon_1^\rho = 30.1$ meV from the top of the valence band ϵ_V, and the amplitude of modulation of the bands is equal to $\epsilon_1^\alpha = 23.1$ meV. High values of the activation energy ϵ_1^α in both semiconductors indicate their strong compensation, which in *p*-type semiconductors can be caused only by free electrons. After all, the position of the Fermi energy ϵ_F is determined by the ratio of the concentrations of ionized acceptors and donors. The question arises about the mechanisms of emergence of donors in $Lu_{1-x}Sc_xNiSb$. If the nature of acceptors is related to the presence of structural defects in the form of vacancies, what is the source of donors? Is it due to the structure of LuNiSb and ScNiSb or the purity of the initial components or the production technology?

Which of the following statements is closer to the truth will be shown by the following results of electrokinetic, energy and magnetic studies of solid

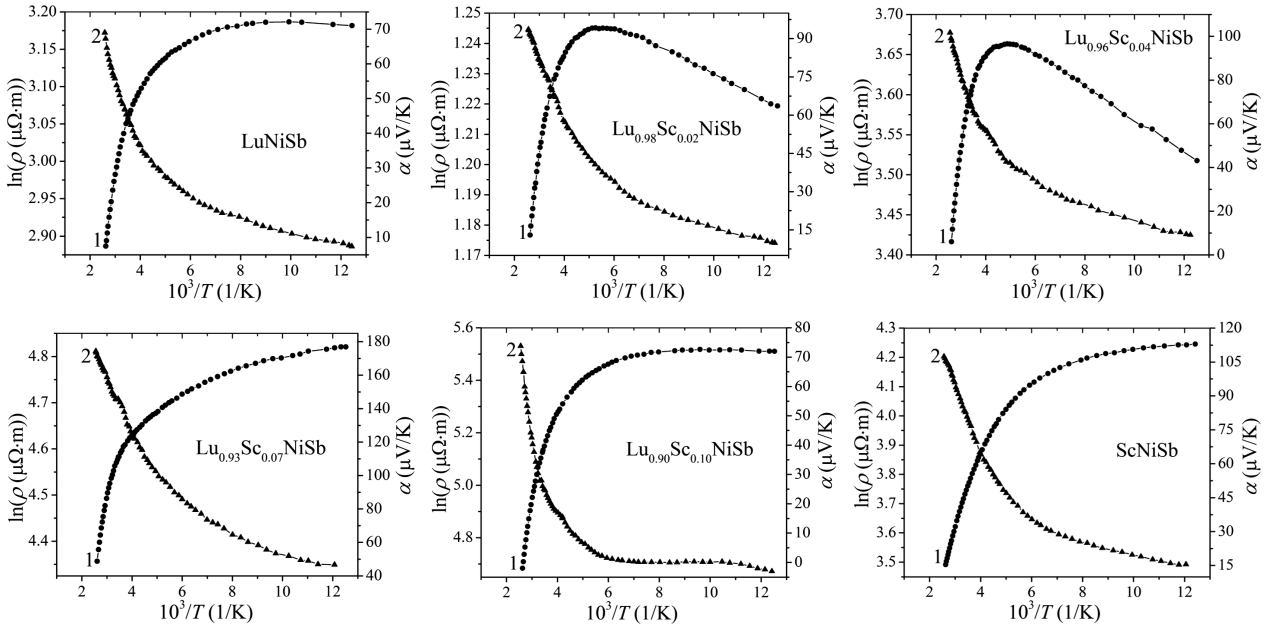

Fig. 5. Temperature dependences of the resistivity $\ln(\rho(1/T, x))$ and thermopower coefficient $\alpha(1/T, x)$ $Lu_{1-x}Sc_xNiSb$

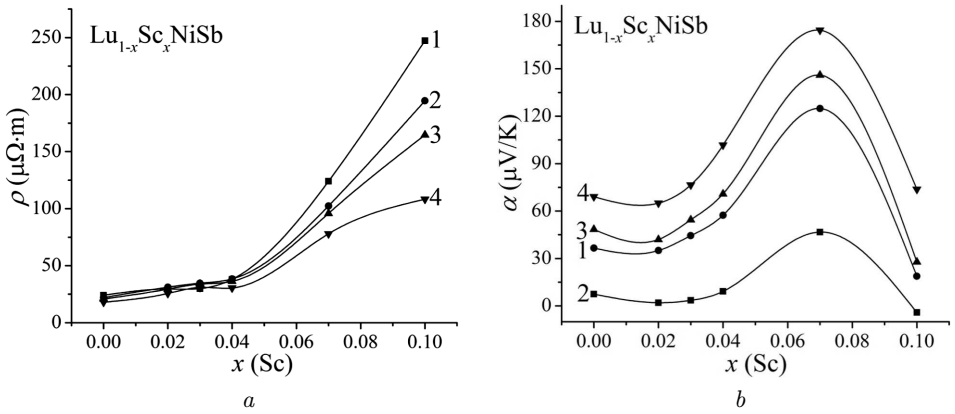

Fig. 6. Variations in the values of the resistivity $\rho(x, T)$ (*a*) and thermopower coefficient $\alpha(x, T)$ (*b*) of the samples $Lu_{1-x}Sc_xNiSb$ at different temperatures: $T = 80$ K (*1*); $T = 250$ K (*2*); $T = 300$ K (*3*); $T = 380$ K (*4*)

solution $Lu_{1-x}Sc_xNiSb$, $x = 0$–0.10, and ScNiSb half-Heusler phase.

3.3. Investigation of electrokinetic and magnetic properties

The temperature and concentration dependences of the resistivity ρ and the thermopower coefficient α for $Lu_{1-x}Sc_xNiSb$, $x = 0$–0.10, and ScNiSb compounds are shown in Figs. 5 and 6. The presence of high- and low-temperature activation parts on the dependences $\ln(\rho(1/T, x))$ and $\alpha(1/T, x)$ (Fig. 5) indicates that the studied samples are doped and compensated semiconductors. The Fermi level ϵ_F is in the band gap ϵ_g, near the valence band ϵ_V, and the holes are the main current carriers, as indicated by the positive values of the thermopower coefficient α (Figs. 5, 6).

Temperature dependences $\ln(\rho(1/T, x))$ for $Lu_{1-x}Sc_xNiSb$ can be described by Eq. (1) [12]:

$$\rho^{-1}(T) = \rho_1^{-1} \exp\left(-\frac{\varepsilon_1^\rho}{k_B T}\right) + \rho_3^{-1} \exp\left(-\frac{\varepsilon_3^\rho}{k_B T}\right), \qquad (1)$$

where the first high-temperature term describes the activation of current carriers $\epsilon_1^\rho(x)$ from the Fermi level ϵ_F to the valence band ϵ_V, and the second, low-temperature term, the jumping conductivity $\epsilon_3^\rho(x)$ with energies close to the Fermi level ϵ_F.

The change in the thermopower coefficient $\alpha(1/T, x)$ with the temperature for $Lu_{1-x}Sc_xNiSb$ (Fig. 5) is described by formula (2) [11]:

$$\alpha = \frac{k_\mathrm{B}}{e}\left(\frac{\varepsilon_V^\alpha}{k_\mathrm{B}T} - \gamma + 1\right), \qquad (2)$$

where γ is a parameter that depends on the nature of the scattering mechanism. From the high- and low-temperature activation parts of the thermopower dependences $\alpha(1/T, x)$ for $Lu_{1-x}Sc_xNiSb$ according to formula (2), the values of activation energies $\epsilon_1^\alpha(x)$ and $\epsilon_3^\alpha(x)$ were calculated, which are proportional to the modulation amplitudes for continuous energy bands and small-scale fluctuations, respectively [13]. The higher the degree of semiconductor compensation, the greater the amplitude of band modulation [12].

Analysis of the temperature dependences $\ln(\rho(1/T, x))$ $Lu_{1-x}Sc_xNiSb$ (Fig. 5) shows that, in some samples, in particular, at $x = 0.02$ and $x = 0.04$, there are no low-temperature activation parts and the mechanism of jumping ϵ_3^ρ-conductivity. In these samples at low temperatures, the values of resistivity ρ increase with the temperature (metallic conductivity). Metallization of low-temperature conductivity indicates the proximity of the Fermi energy ϵ_F and the percolation level of the valence band ϵ_V, which facilitates the ionization of acceptors and the appearance of free holes in it. We can assume that, in samples $Lu_{1-x}Sc_xNiSb$, $x = 0.01$–0.04, at low temperatures, there is a significant number of ionized acceptors, which leads to overlapping of the wave functions of impurity states near the Fermi energy ϵ_F. In this case, the impurity acceptor band intersects with the valence band ϵ_V, forming a "tail".

At the same time, in the samples of LuNiSb, $Lu_{0.93}Sc_{0.07}NiSb$, $Lu_{0.90}Sc_{0.10}NiSb$ and ScNiSb compositions at low temperatures, the electrical conductivity is determined by the jumps of the carriers on localized states within the Fermi energy ϵ_F. The fact of the existence of hopping ϵ_3^ρ-conductivity in p-type semiconductors with a significant concentration of acceptors (vacant nature of defects in the structure of LuNiSb and ScNiSb [1, 8, 19]) is possible only in the presence of donors.

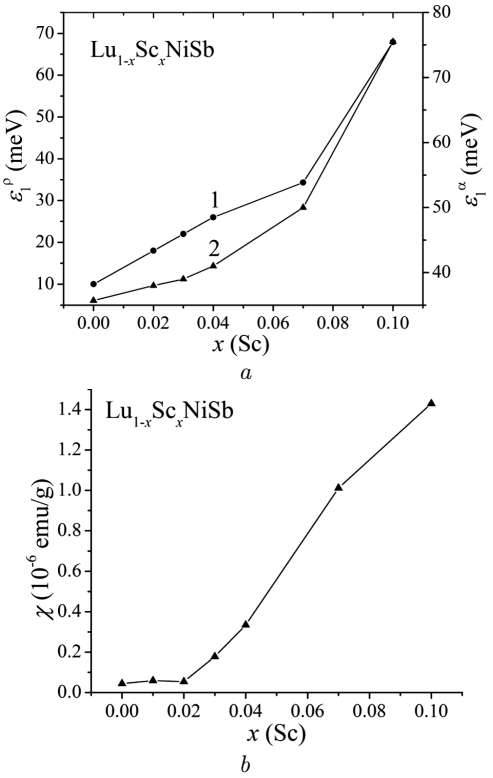

Fig. 7. Variations in the values of activation energies $\epsilon_1^\rho(x)$ (1) and $\epsilon_1^\alpha(x)$ (2) (*a*) and the specific magnetic susceptibility $\chi(x)$ (*b*) $Lu_{1-x}Sc_xNiSb$

In this context, a logical question arises about the mechanisms of donor generation in a p-type semiconductor, provided that it is doped with a neutral impurity. It is clear that the answer is related to the change in the electronic structure of $Lu_{1-x}Sc_xNiSb$ as a result of transformations in the crystal structure when Sc atoms enter the semiconductor matrix. The mechanism of such structural changes in $Lu_{1-x}Sc_xNiSb$ will be shown below.

An important proof of donor generation during p-LuNiSb doping with a neutral Sc impurity is the Fermi energy ϵ_F behavior in $Lu_{1-x}Sc_xNiSb$, $x = 0$–0.10. The variations in the values of the activation energy ϵ_1^ρ of holes from the Fermi level ϵ_F to the valence band ϵ_V (positive values of the thermopower coefficient $\alpha(x, T)$) are shown in Fig. 7, *a*. Therefore, doping p-LuNiSb by a neutral impurity Sc leads to a drift of the Fermi level ϵ_F from the valence band ϵ_V to the middle of the band gap ϵ_g in $Lu_{1-x}Sc_xNiSb$. Thus, if in p-LuNiSb the Fermi level ϵ_F was at a distance of 10.2 meV from the top of the valence band ϵ_V, then

in the case of $Lu_{0.90}Sc_{0.10}NiSb$ it is at a distance of 67.9 meV. In a semiconductor, this is possible, only if the number of donors increases or the number of acceptors decreases with a constant number of donors.

Analysis of the behavior of the activation energy $\epsilon_1^{\rho}(x)$ for $Lu_{1-x}Sc_xNiSb$, $x = 0$–0.10, from the Fermi level ϵ_F to the valence band ϵ_V shows that, in the concentration interval $x = 0$–0.07, the dependence is almost linear (Fig. 7, *a*, curve *1*). This allows us to determine the motion rate of the Fermi level ϵ_F, which is $\Delta\epsilon_F/\Delta x \approx 4.9$ meV/%Sc. From concentrations ≥ 0.07, the angle of inclination $\epsilon_1^{\rho}(x)$ increases, indicating an increase in rate to $\Delta\epsilon_F/\Delta x \approx \approx 11.2$ meV/%Sc. The fact that, for two concentration intervals, the motion rates of the Fermi level ϵ_F differ by ~ 2 times indicates different changes in the crystal structure of $Lu_{1-x}Sc_xNiSb$. Therefore, at these concentrations, the rates of generation of structural defects of acceptor and donor natures are different.

Another proof that donors are generated in $Lu_{1-x}Sc_xNiSb$ is the nature of the variation in the values of the activation energy $\epsilon_1^{\alpha}(x)$, calculated from the high-temperature parts of the thermopower coefficient $\alpha(1/T, x)$ for $Lu_{1-x}Sc_xNiSb$ (Fig. 7, *a*, curve *2*). Activation energies $\epsilon_1^{\alpha}(x)$ are proportional to the amplitude of modulation of continuous energy bands and are related to the degree of semiconductor compensation [13]. Therefore, the nature of the behavior of $\epsilon_1^{\alpha}(x)$ can be judged on the ratio of ionized acceptors and donors. Thus, in *p*-LuNiSb, the amplitude of modulation of the continuous energy bands is equal to $\epsilon_1^{\alpha} \approx 35.7$ meV, and, at the concentration $x = 0.02$ – $\epsilon_1^{\alpha}(x = 0.02) \approx 39.1$ meV, showing an increase in the compensation degree. At higher Sc concentrations, the activation energy increases from $\epsilon_1^{\alpha}(x = 0.04) \approx 41.2$ meV to $\epsilon_1^{\alpha}(x = = 0.07) \approx 50.1$ meV and $\epsilon_1^{\alpha}(x = 0.10) \approx 75.4$ meV. In a *p*-type semiconductor, an increase in the degree of compensation (the ratio of ionized acceptors and donors) is possible, only if the concentration of donors increases [12]. Thus, the increase in the compensation degree of $Lu_{1-x}Sc_xNiSb$ semiconductor experimentally proves the existence of a mechanism of generation of structural defects of donor nature of the unknown origin.

Let us try to identify the nature of donors.

In the course of studying the structural and energy characteristics of $Lu_{1-x}Sc_xNiSb$, it was stated that Sc atoms occupy vacancies in 4*a* position, which simultaneously eliminates structural defects of acceptor nature and the corresponding acceptor band. At the same time, the structural defects of donor nature are formed with the appearance of the corresponding donor band ϵ_D^1 in the band gap ϵ_g, which supplies free electrons, by making the $Lu_{1-x}Sc_xNiSb$ semiconductor highly doped and compensated. This mechanism of structural changes in $Lu_{1-x}Sc_xNiSb$, which generates the appearance of the donor band ϵ_D^1, is the most real and consistent with the results of electrokinetic and energy studies. Thus, the peculiarity of the mechanism of electrical conductivity of $Lu_{1-x}Sc_xNiSb$ at different concentrations is the different rates of generation of structural defects of acceptor and donor natures, due to the corresponding structural changes. This statement provides an answer to the main purpose of the study – to establish the features of the mechanisms of electrical conductivity $Lu_{1-x}Sc_xNiSb$.

The experimental results of variations in the values of the resistivity $\rho(x, T)$, thermopower coefficient $\alpha(x, T)$ (Fig. 6), and Fermi energy ϵ_F (Fig. 7, *a*, curve *1*) are consistent with the results of experimental measurements of the specific magnetic susceptibility $\chi(x)$ $Lu_{1-x}Sc_xNiSb$, $x = 0$–0.10, at room temperature (Fig. 7, *b*). The studies have shown that the $Lu_{1-x}Sc_xNiSb$ semiconductor is a Pauli paramagnet in which the magnetic susceptibility is determined exclusively by the electron gas and is proportional to the density of states at the Fermi level ϵ_F. As can be seen from Figs. 7, *b*, the dependence $\chi(x)$, as well as $\rho(x, T)$, $\alpha(x, T)$ and $\epsilon_F(x)$, slightly changes in the interval of concentrations $x = 0$–0.02, which we associate with a small concentration of free electrons generated by the formed donor band ϵ_D^1. At higher concentrations of Sc, the rate of change in the magnetic susceptibility $\chi(x)$ for $Lu_{1-x}Sc_xNiSb$, as well as $\rho(x, T)$, $\alpha(x, T)$ (Fig. 6) and $\epsilon_F(x)$ (Fig. 7, *a*, curve *1*) increases, showing an increase in the rate of generation of free electrons.

4. Conclusions

The omprehensive study of the crystal and electronic structures, thermodynamic, electrokinetic, energy, and magnetic properties of the semiconductive solid solution $Lu_{1-x}Sc_xNiSb$, $x = 0$–0.10, has revealed the possibility of occupying impurity Sc different crystallographic positions depending on their concentration. This leads to the generation of structural defects

of donor and/or acceptor nature and the appearance of the corresponding energy levels (bands) in the band gap ϵ_g. The ratio of ionized donors and acceptors (degree of compensation) determines the position of the Fermi level ϵ_F in $Lu_{1-x}Sc_xNiSb$. The dependence of the rate of generation of energy levels and the position of the Fermi level ϵ_F on the impurity concentration of Sc, which determines the mechanism of electrical conductivity $Lu_{1-x}Sc_xNiSb$, is established. The investigated solid solution $Lu_{1-x}Sc_xNiSb$ is a promising thermoelectric material.

We would like to acknowledge financial support of the Ministry of Education and Science of Ukraine under grant No. 0121U109766.

1. I. Karla, J. Pierre, R.V. Skolozdra. Physical properties and giant magnetoresistance in RNiSb compounds. *J. Alloys Compd.* **265**, 42 (1998).
2. V.V. Romaka, L. Romaka, A. Horyn, P. Rogl, Yu. Stadnyk, N. Melnychenko, M. Orlovskyy, V. Krayovskyy. Peculiarities of thermoelectric half-Heusler phase formation in Gd–Ni–Sb and Lu–Ni–Sb ternary systems. *J. Solid State Chem.* **239**, 145 (2016).
3. V.V. Romaka, L. Romaka, A. Horyn, Yu. Stadnyk. Experimental and theoretical investigation of the Y–Ni–Sb and Tm–Ni–Sb systems. *J. Alloys Compd.* **855**, 157334 (2021).
4. K. Hartjes, W. Jeitschko. Crystal structure and magnetic properties of the lanthanoid nickel antimonides LnNiSb (Ln = La–Nd, Sm, Gd–Tm, Lu). *J. Alloys Compd.* **226**, 81 (1995).
5. V.A. Romaka, Yu. Stadnyk, L. Romaka, V. Krayovskyy, A. Horyn, P. Klyzub, V. Pashkevych. Study of structural, electrokinetic and magnetic characteristics of the $Er_{1-x}Zr_xNiSb$ Semiconductor. *J. Phys. Chem. Sol. State.* **21**, 689 (2020).
6. V.A. Romaka, Yu.V. Stadnyk, L.P. Romaka, V.Z. Pashkevych, V.V. Romaka, A.M. Horyn, P.Yu. Demchenko. Study of structural, thermodynamic, energy, kinetic and magnetic properties of thermoelectric material $Lu_{1-x}Zr_xNiSb$. *J. Thermoelectricity.* **1**, 32 (2021).
7. V.A. Romaka, Yu. Stadnyk, L. Romaka, A. Horyn, V. Pashkevych, H. Nychyporuk, P. Garanyuk. Investigation of thermoelectric material based on $Lu_{1-x}Zr_xNiSb$ solid solution. I. Experimental Results. *J. Phys. Chem. Sol. State.* **23**, 235 (2022).
8. V.A. Romaka, Yu.V. Stadnyk, V.Ya. Krayovskyy, L.P. Romaka, O.P. Guk, V.V. Romaka, M.M. Mykyychuk, A.M. Horyn. *The Latest Heat-Sensitive Materials and Temperature Transducers* (Lviv Polytechnic Publishing House, 2020) [in Ukrainian] [ISBN 978-966-941-478-6].
9. V.A. Romaka, Yu. Stadnyk, L. Romaka, V. Krayovskyy, P. Klyzub, V. Pashkevych, A. Horyn, P. Garanyuk. Synthesis and electrical transport properties of $Er_{1-x}Sc_xNiSb$ semiconducting solid solution. *J. Phys. Chem. Sol. State.* **22**, 146 (2021).
10. I. Wolacska, K. Synoradzki, K. Ciesielski, K. Zaikski, P. Skokowski, D. Kaczorowski. Enhanced thermoelectric power factor of half-Heusler solid solution $Sc_{1-x}Tm_xNiSb$ prepared by high-pressure high-temperature sintering method. *Mater. Chem. and Phys.* 29 (2019).
11. N.F. Mott, E.A. Davis. *Electron Processes in Non-Crystalline Materials* (Clarendon Press, 1979).
12. B.I. Shklovskii, A.L. Efros. *Electronic properties of doped semiconductors* (Springer, 1984).
13. V.A. Romaka, E.K. Hlil, Ya.V. Skolozdra, P. Rogl, Yu.V. Stadnyk, L.P. Romaka, A.M. Goryn. Features of the mechanisms of generation and "Healing" of structural defects in the heavily doped intermetallic semiconductor *n*-ZrNiSn. *Semiconductors.* **43**, 1115 (2009).
14. V.P. Babak, V.V. Shchepetov. Wear resistance of amorphous-crystalline coatings with lubricants. *J. Friction and Wear.* **39**, 38 (2018).
15. T. Roisnel, J. Rodriguez-Carvajal. WinPLOTR: A windows tool for powder diffraction patterns analysis. *Mater. Sci. Forum*, Proc. EPDIC7 378-381 (2001).
16. V.L. Moruzzi, J.F. Janak, A.R. Williams. *Calculated Electronic Properties of Metals* (Pergamon Press, 1978).
17. H. Akai. Fast Korringa–Kohn–Rostoker coherent potential approximation and its application to FCC Ni–Fe systems. *J. Phys.: Condens. Matter.* **1**, 8045 (1989).
18. The Elk code An all-electron full-potential linearised augmented-plane wave (LAPW) code. http://elk.sourceforge.net.
19. K. Synoradzki, K. Ciesielski, I. Veremchuk, H. Borrmann, P. Skokowski, D. Szymanski, Y. Grin, D. Kaczorowski. Thermal and electronic transport properties of the Half-Heusler phase ScNiSb. *Materials.* **12**, 1723 (2019).

Received 30.05.22

В.В. Ромака, В.А. Ромака, Ю.В. Стадник,
Л.П. Ромака, П.Ю. Демченко, В.З. Пашкевич, А.М. Горинь

ОСОБЛИВОСТІ МЕХАНІЗМІВ ЕЛЕКТРОПРОВІДНОСТІ НАПІВПРОВІДНИКОВОГО ТВЕРДОГО РОЗЧИНУ $Lu_{1-x}Sc_xNiSb$

Комплексне дослідження кристалічної та електронної структур, термодинамічних, кінетичних, енергетичних та магнітних властивостей напівпровідникового твердого розчину $Lu_{1-x}Sc_xNiSb$, x = 0–0,10, виявило можливість зайняття легуючими атомами Sc різних кристалографічних позицій у залежності від їхньої концентрації. Це приводить до генерування структурних дефектів донорної і/або акцепторної природи та появи у забороненій зоні ϵ_g відповідних енергетичних рівнів (зон). Співвідношення іонізованих донорів та акцепторів (ступінь компенсації) визначає у $Lu_{1-x}Sc_xNiSb$ положення рівня Фермі ϵ_F. Встановлено залежність швидкості генерування енергетичних рівнів та положення рівня Фермі ϵ_F від концентрації домішки Sc, що визначає механізм електропровідності $Lu_{1-x}Sc_xNiSb$. Досліджений твердий розчин $Lu_{1-x}Sc_xNiSb$ є перспективним термоелектричним матеріалом.

Ключові слова: електропровідність, коефіцієнт термо-е.р.с., рівень Фермі, напівпровідник.